Lamellar Ordering in Symmetric Diblock Copolymers

R. A. Sones,* E. M. Terentjev, and R. G. Petschek

Department of Physics, Case Western Reserve University, Cleveland, Ohio 44106-7079

Received November 12, 1992; Revised Manuscript Received March 1, 1993

ABSTRACT: We calculate the lamellar period L and interphase thickness a of an incompressible melt of symmetric diblock copolymers from the onset of phase segregation (weak segregation limit) to the limit where segregation is almost complete (strong segregation limit) by numerically solving a mean field lattice model, where the lattice spacing is taken small enough to approximate a continuum. Our results for L and a agree with previously derived theoretical formulas in both limits. Based on the first few terms of a Fourier series expansion of the density profile, we show analytically that $L = 0.844R(\chi N)^{0.571}$ at the weak segregation limit, where R is the unperturbed molecular radius of gyration, χ the Flory interaction parameter, and N the number of statistical segments per molecule; the compressibility of the melt—even in the incompressible limit—must be taken into consideration to get the correct dependence of L on χN, and the Fourier series approximation turns out to be accurate over a very small range of χN.

I. Introduction

A polymer is called a diblock copolymer if it consists of two subchains (or blocks), one containing type A monomers and the other type B. Typically A and B monomers have a positive free energy of mixing when the translation entropy—which is small for monomers constrained to be on a polymer—is ignored, and in a melt they tend to segregate into A-rich and B-rich domains. The linkage between A and B blocks precludes macroscopic phase separation and leads to interesting microscopic ordering on a scale of the radius of gyration of the polymer. A recent article by Bates[1] reviews polymer–polymer phase behavior and references much of the literature.

Theorists resort to various approximations when describing diblock copolymer melts. The molecules are typically modeled as ideal Gaussian chains with the same Kuhn length and volume per monomer for both blocks, and usually the melt is assumed incompressible. The statistical mechanics of this simplified model is then solved by the application of mean field theory or the random phase approximation.

Within the framework of these approximations, analytic descriptions of microphase ordering have been proposed for two limiting cases. A melt of symmetric (same number of monomers in both blocks) diblock copolymers, with N monomers per molecule, unperturbed radius of gyration R, and Flory interaction parameter χ (which is approximately inversely proportional to temperature), is expected to exhibit a transition from a homogeneous mixture to an ordered structure when χN exceeds 10.5.[2] In the weak segregation limit ($\chi N \simeq 10.5$) the density distribution exhibits shallow sinusoidal modulation with predicted period $3.23R$.[2] As χN increases the modulation depth and period increase, until in the strong segregation limit ($\chi N \gg 10.5$) the density distribution is lamellar with predicted period[3]

$$L = (192/\pi^2)^{1/3}R(\chi N)^{1/6} \tag{1}$$

In this limit the predicted size of the transition region between A and B phases (the interphase width) is[3,4]

$$a = 2R(\chi N)^{-1/2}\left[1 + \frac{4}{\pi}\left(\frac{3}{\pi^2\chi N}\right)^{1/3}\right] \tag{2}$$

where the second term in brackets is a correction recently derived by Semenov.[5] The interphase width is defined as the peak-to-peak modulation of the type A (or type B) density distribution divided by the magnitude of its slope at the center of the transition region. According to this definition, at the weak segregation limit where the density distribution is sinusoidal, the interphase width is $3.23R/\pi$.

No analytic expressions exist for L or a for intermediate values of χN. In an early paper on block copolymers, Helfand[6] numerically calculated density distributions for $\chi N = 20$ and 74, from which values of L and a can be extracted. Recently, Melenkevitz and Muthukumar[7] and Shull[8] numerically calculated L for the entire range of χN from the weak to the strong segregation limits. Both find $L \sim R(\chi N)^{1/6}$ in the strong segregation limit, and $L = 3.23R$ at the weak segregation limit, but in the intermediate regime their results disagree. Shull discusses this disagreement and argues that his calculation involves fewer assumptions. Shull's results for L converge to eq 1 in the strong segregation limit; this is reassuring, since his calculations are based on the same mean field theory for which eq 1 was derived. Shull also numerically calculated a and compared his results to eq 2 without the correction term and found about 10% disagreement well into the strong segregation regime ($\chi N \simeq 150$); inclusion of the correction term eliminates this disagreement.

The dependence of L on χN in the weak segregation limit is a topic of current interest. The belief is widespread that $L \sim R$ in this limit,[7,9] but some measurements[10] suggest $L \sim RN^{0.3}$, one recent theory[11] predicts $L \sim RN^{0.5}$, and Shull[8] deduces $L \sim RN^{0.45}$ from his numerical data.

In this paper we calculate L and a for χN ranging from the weak to the strong segregation limits, by numerically solving a mean field model implemented on a lattice—an approach similar to that of Shull.[8] Then in section III.A we show analytically that our model yields $L = 0.844R(\chi N)^{0.571}$ in the weak segregation limit.

II. Mean Field Theory

Our mean field model is similar to that of Helfand,[4,6,12] but our notation and approximations are geared for direct numerical solution. Consider a system of volume V and temperature T (in energy units) containing N_c identical noninteracting diblock copolymer molecules. We regard each molecule as a freely-jointed chain with N segments and treat space as a simple cubic lattice with lattice constant l, where l^3 is the mean volume per segment, and require adjacent molecular segments to occupy nearest-neighbor lattice sites.[13] $\mathcal{N} = V/l^3$ is the total number of lattice sites. As $l \to 0$ the cubic lattice approaches a continuum and the freely-jointed chains become ideal

0024-9297/93/2226-3344$04.00/0

Gaussian chains; in our calculations we will take l small enough so that its size does not affect our results. (Though our interest in this paper is with symmetric diblock copolymers, the theory we present in this section does not assume both blocks have the same number of segments. However, we do assume the blocks have the same Kuhn length and volume per segment.)

Let $i = A, B$ be the block index, $k = 1, 2, ..., N$ the segment index, and i_k the value of the block index of the kth segment. When the chains are acted upon by a mean field $\mu(i,\mathbf{r})$, which gives the energy per unit temperature of a type i segment at lattice site $\mathbf{r}$, the system partition function (neglecting constant factors) is

$$Z = Z_c^{N_c} \tag{3}$$

where Z_c is the single-chain partition function (see, for example, eq 2.1 of ref 4)

$$Z_c = \sum_{\mathbf{r}_1} \cdots \sum_{\mathbf{r}_N} \exp(-\sum_k \mu(i_k,\mathbf{r}_k)) \times P(\mathbf{r}_1 - \mathbf{r}_2) \cdots P(\mathbf{r}_{N-1} - \mathbf{r}_N) \tag{4}$$

and the summations before the exponential are over all lattice sites. $P(\mathbf{r}_{k-1} - \mathbf{r}_k)$ is the probability that segment k is located at $\mathbf{r}_k$ when segment $k-1$ is at $\mathbf{r}_{k-1}$. For a random walk on a cubic lattice

$$P(\mathbf{r}) = \begin{cases} 1/6 & \text{if } \mathbf{r} = \pm l\hat{\mathbf{x}}, \pm l\hat{\mathbf{y}}, \pm l\hat{\mathbf{z}} \\ 0 & \text{otherwise} \end{cases} \tag{5}$$

where $\hat{\mathbf{x}}$, $\hat{\mathbf{y}}$, and $\hat{\mathbf{z}}$ are unit vectors. When $N \gg 1$, this random walk results in a Gaussian distribution for the distance between chain ends with variance $2R^2$, where $R^2 = (N/6)l^2$.[13] Equation 4 can be written

$$Z_c = \sum_{\mathbf{r}} Z^0(k,\mathbf{r}) \tag{6}$$

where

$$Z^0(k,\mathbf{r}) = Z^-(k,\mathbf{r}) \exp(-\mu(i_k,\mathbf{r}))Z^+(k,\mathbf{r}) \tag{7}$$

$$Z^\pm(k,\mathbf{r}) = \sum_{\mathbf{r}'} P(\mathbf{r}' - \mathbf{r}) \exp(-\mu(i_k,\mathbf{r}'))Z^\pm(k\pm1,\mathbf{r}') \tag{8}$$

and at the chain ends

$$Z^-(1,\mathbf{r}) = Z^+(N,\mathbf{r}) = 1 \tag{9}$$

$Z^0(k,\mathbf{r})$ is the statistical weight (unnormalized probability) of finding segment k of a given chain at $\mathbf{r}$, and $Z^\pm(k,\mathbf{r})$ are the statistical weights associated with the portions of the chain before (−) and after (+) segment k. Given $\mu(i,\mathbf{r})$, the recursive structure of eq 8 allows one to calculate $Z^0(k,\mathbf{r})$ and Z_c from eqs 5–9.

Now consider interactions between segments. In the spirit of Flory–Huggins theory write the local free energy density

$$f(\mathbf{r}) = T\rho_0\left(\frac{(\phi(\mathbf{r}) - 1)^2}{2\kappa} + \chi\phi(A,\mathbf{r})\phi(B,\mathbf{r})\right) \tag{10}$$

where κ is a dimensionless compressibility, χ the Flory interaction parameter for A and B segments, $\rho_0 = N_cN/V$ the mean number density of segments, and $\phi(i,\mathbf{r})$ the number of type i segments per lattice site at $\mathbf{r}$. Here $\phi(i,\mathbf{r})$ is a reduced (dimensionless) partial density, while the total density is

$$\phi(\mathbf{r}) = \sum_i \phi(i,\mathbf{r}) \tag{11}$$

(Our $f(\mathbf{r})$ is identical to that used by Helfand in ref 12. Slightly different forms are used in other papers, but they all give identical results for polymer melts in the incompressible limit.[14]) We approximate the free energy (per chain per unit temperature) of a system of interacting chains as

$$\mathcal{F} = -\ln(Z_c) - \frac{N}{\mathcal{N}}\sum_i\sum_{\mathbf{r}}\mu(i,\mathbf{r})\phi(i,\mathbf{r}) + \frac{N}{\mathcal{N}}\sum_{\mathbf{r}}\left(\frac{(\phi(\mathbf{r}) - 1)^2}{2\kappa} + \chi\phi(A,\mathbf{r})\phi(B,\mathbf{r})\right) \tag{12}$$

where the first term on the right is the total free energy of a system of chains in the presence of the mean field but without segment–segment interactions (the reference state), the second is the free energy of the reference state due to interactions between segments and the mean field, and the third is the Flory–Huggins free energy evaluated in the reference state.[15] The first and second terms give the entropy of the reference state, which makes it clear that we are simply using the entropy of the reference state (which we know how to calculate) as an approximation for the entropy of the interacting state. This procedure gives an upper bound to the free energy. The "best" such free energy is then given by functional minimization of eq 12 with respect to both ϕ and μ, resulting in the equations

$$\mu(A,\mathbf{r}) = \frac{\phi(\mathbf{r}) - 1}{\kappa} + \chi\phi(B,\mathbf{r}) \tag{13}$$

$$\mu(B,\mathbf{r}) = \frac{\phi(\mathbf{r}) - 1}{\kappa} + \chi\phi(A,\mathbf{r}) \tag{14}$$

$$\phi(i,\mathbf{r}) = \frac{\mathcal{N}}{N}\sum_k \delta(i,i_k)\frac{Z^0(k,\mathbf{r})}{Z_c} \tag{15}$$

where the Kronecker delta function restricts the summation to segments in block i. Equations 13 and 14 come from variational terms containing $\delta\phi$, while eq 15 comes from terms containing $\delta\mu$. Variation of $\ln(Z_c)$ is facilitated by noting that

$$\delta Z_c = -\sum_k\sum_{\mathbf{r}} Z^0(k,\mathbf{r})\delta\mu(i_k,\mathbf{r}) \tag{16}$$

Equations 6 and 15 imply the average value of $\phi(\mathbf{r})$ is unity.

Based on a mean field approximation and the Flory–Huggins local free energy density, eqs 13–15 give a formal solution for a diblock copolymer system. The goal is to find distributions ϕ and μ which satisfy eqs 13–15 when Z^0 and Z_c are calculated from eqs 5–9.

III. Solution Methods

A. Analytic Solution near the Weak Segregation Limit. In this section we investigate the behavior of our model for symmetric blocks near the weak segregation limit ($\chi N \simeq 10.5$) when $N \to \infty$ and $\chi \to 0$. Near the weak segregation limit the density profiles are one-dimensional sinusoids with infinitesimal amplitude,[2] and we write

$$\phi(A,z) = \frac{1}{2}(1 + \epsilon\cos(qz) + \tau\epsilon^2\cos(2qz)) \tag{17}$$

$$\phi(B,z) = \frac{1}{2}(1 - \epsilon\cos(qz) + \tau\epsilon^2\cos(2qz)) \tag{18}$$

where $q \equiv 2\pi/L$, z is the position coordinate normal to the lamellae, $\epsilon \ll 1$, and the signs are dictated by symmetry since $\phi(A,z+L/2) = \phi(B,z)$ for symmetric blocks. Given eqs 17 and 18, we will derive an expression for the free energy in terms of q, ϵ, and τ, then minimize this free

energy to determine equilibrium values of q, ϵ, and τ as functions of χN. Since we are interested in calculating properties in the neighborhood of the weak segregation limit, we keep only the two leading terms (ϵ^2 and ϵ^4) in the free energy. Terms of higher order than ϵ^2 have been neglected in eqs 17 and 18 because they contribute terms of higher order than ϵ^4 to the free energy.

From eq 11 we find

$$\phi(z) = 1 + \tau\epsilon^2 \cos(2qz) \tag{19}$$

then eq 13 gives

$$\mu(A,z) = \frac{\chi}{2}(1 - \epsilon \cos(qz) + \omega\tau\epsilon^2 \cos(2qz)) \tag{20}$$

where

$$\omega \equiv 1 + \frac{2}{\chi\kappa} \tag{21}$$

(Note that eq 19 describes a compressible melt, even though we intend to eventually calculate results when κ and τ go to zero. See the related discussion in section IV.) $\mu(B,z)$ is obtained from $\mu(A,z)$ by replacing ϵ with $-\epsilon$. As $N \to \infty$ the lattice sums in eq 12 become integrals, and, using the orthogonality of the cosines, the free energy is

$$\mathcal{F} = -\ln(Z_c) - \frac{1}{4}\chi N + \frac{1}{8}\chi N\epsilon^2 - \frac{1}{32\omega}\tilde{\tau}^2(\chi N)^3\epsilon^4 \tag{22}$$

where

$$\tilde{\tau} \equiv \frac{2\omega\tau}{\chi N} \tag{23}$$

The calculation of $\ln(Z_c)$ is tedious and is outlined in Appendix A. The result is

$$\ln(Z_c) = -\frac{1}{2}\chi N + a_1(\chi N)^2\epsilon^2 - \left(\frac{1}{2}a_1^2 - a_2 - a_3\tilde{\tau} - a_4\tilde{\tau}^2\right)(\chi N)^4\epsilon^4 \tag{24}$$

where the coefficients a_1, a_2, a_3, and a_4 are functions of $\tilde{q} \equiv qR$ and are given in Appendix A. Equations 22 and 24 give

$$\Delta\mathcal{F} = \frac{1}{8}\left(\frac{1}{\chi N} - 8a_1\right)(\chi N)^2\epsilon^2 + \left(\frac{1}{2}a_1^2 - a_2 - a_3\tilde{\tau} - a_4\tilde{\tau}^2\right)(\chi N)^4\epsilon^4 \tag{25}$$

where $\Delta\mathcal{F} \equiv \mathcal{F} - \chi N/4$, and we have made the approximation $(a_4 + 1/(32\omega\chi N)) \simeq a_4$ since we are interested in the limit $\omega \to \infty$ as $\chi \to 0$ with χN finite. Minimizing the right-hand side of eq 25 with respect to $\tilde{q}$, ϵ, and $\tilde{\tau}$ gives

$$\chi N = \frac{1}{8}\left(\frac{b'(\tilde{q}_0)}{a_1(\tilde{q}_0)b'(\tilde{q}_0) - 2a_1'(\tilde{q}_0)b(\tilde{q}_0)}\right) \tag{26}$$

$$\epsilon_0^2 = \frac{1}{16(\chi N)^3}\left(\frac{8a_1(\tilde{q}_0)\chi N - 1}{b(\tilde{q}_0)}\right) \tag{27}$$

$$\tilde{\tau}_0 = -\frac{a_3(\tilde{q}_0)}{2a_4(\tilde{q}_0)} \tag{28}$$

$$\Delta\mathcal{F}_0 = -\frac{1}{256(\chi N)^2}\left(\frac{8a_1(\tilde{q}_0)\chi N - 1}{b(\tilde{q}_0)}\right) \tag{29}$$

where the subscript zero denotes a value at equilibrium, the primes denote differentiation with respect to $\tilde{q}$, and

$$b \equiv \frac{1}{2}a_1^2 - a_2 + \frac{a_3^2}{4a_4} \tag{30}$$

Since $L_0 = 2\pi R/\tilde{q}_0$, eq 26 determines L_0 as a function of χN.

The results of Leibler[2] are recovered if we set $\epsilon_0 = 0$ in eq 27, which gives $\chi N = 1/(8a_1(\tilde{q}_0))$. The function $a_1(\tilde{q}_0)$ has a maximum at $\tilde{q}_0 = 1.946$, corresponding to the disorder–order transition at $\chi N = 10.5$.

As discussed in section I, near the weak segregation limit L is commonly written in the form $L \sim RN^{\alpha}$. By numerically evaluating eq 26 in the neighborhood of the disorder–order transition, we find

$$L = 0.844R(\chi N)^{0.571} \tag{31}$$

B. Numerical Solution Strategy. In this section we describe a numerical procedure for finding the distributions ϕ and μ for arbitrary χN. For a given density distribution ϕ, one can calculate the corresponding field μ from eqs 13 and 14 and then a new density distribution $\mathbf{T}\phi$ from eqs 5–9 and 15. Here $\mathbf{T}$ is an operator representing the transformation of the density distribution. Think of ϕ and $\mathbf{T}\phi$ as points in a space spanned by $\{i,\mathbf{r}\}$, and consider the difference vector $\mathbf{T}\phi - \phi$. Define the length Δ of the difference vector by

$$\Delta^2[\phi] \equiv \frac{1}{2\mathcal{N}}\sum_i\sum_{\mathbf{r}}(\mathbf{T}\phi(i,\mathbf{r}) - \phi(i,\mathbf{r}))^2 \tag{32}$$

If ϕ is an exact solution, then $\phi = \mathbf{T}\phi$ and $\Delta = 0$. Otherwise, $\Delta > 0$. The closer Δ is to zero, the closer ϕ is to an exact solution. Δ is a scalar field, and one can use standard multidimensional minimization techniques (such as conjugate gradient descent[16]) to locate the solution point where $\Delta = 0$. However, we use the following approach, which we have found to be simpler and more efficient.

Guess an initial ϕ and consider the line passing through ϕ in the direction $\mathbf{T}\phi - \phi$. This line may be written

$$\tilde{\phi}(i,\mathbf{r};\nu) = \phi(i,\mathbf{r}) + \nu(\mathbf{T}\phi(i,\mathbf{r}) - \phi(i,\mathbf{r})) \tag{33}$$

where $\tilde{\phi}$ is a point on the line located "distance" ν from ϕ. Every point on the line has a corresponding Δ given by eq 32. Use standard one-dimensional minimization techniques (such as Brent's method[17]) to find the point on the line with minimum Δ (i.e., minimize Δ with respect to ν), then use this point as an improved new guess. This procedure can be iterated until Δ approaches zero. If at some step during iteration the minimum Δ occurs at $\nu = 0$, convergence fails, and a different initial ϕ should be chosen.

The numerical solution strategy presented in this section is quite general, valid for three-dimensional distributions of asymmetric diblock copolymers. Specialization to the case of one-dimensional (lamellar) structure and symmetric blocks is discussed in Appendix B.

IV. Results and Discussion

Equations 1 and 2 for L and a in the strong segregation limit depend only on χN and R, not the number of segments N. These equations were derived for $N \to \infty$. Similarly, our numerical results for L and a depend only on χN and R when $N \gg 1$, and we have taken N large enough so that the dependence on N is negligible (see Appendix B).

A polymer melt is nearly incompressible ($\kappa \simeq 0$). As $\kappa \to 0$ our numerical results for L and a approach limiting values corresponding to an incompressible system (see Figure 1). In the following numerical calculations we used $\kappa = 0.1$ to simulate an incompressible system. Reducing

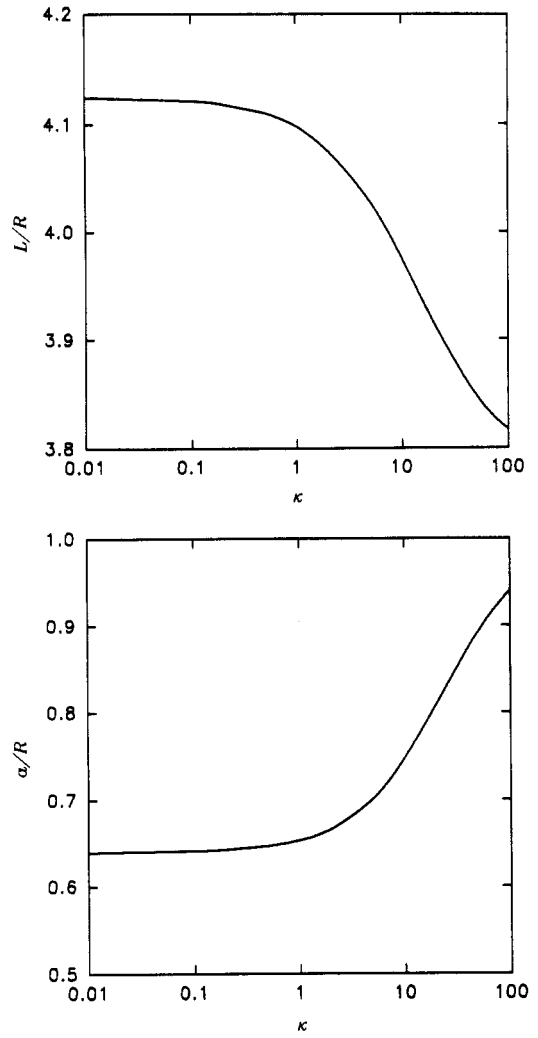

Figure 1. Dependence of (a, top) lamellar period and (b, bottom) interphase width on compressibility ($\chi N = 21$, $N = 210$). For $\kappa \ll 1$ both L and a approach the values they have in an imcompressible system.

Table I. Numerically Calculated Values of L/R and a/R for Given χN

χN	L/R	a/R	χN	L/R	a/R
11.0	3.30	0.992	26.4	4.36	0.551
11.5	3.37	0.963	29.6	4.48	0.512
12.0	3.43	0.934	33.2	4.59	0.476
12.6	3.51	0.903	37.2	4.71	0.444
13.0	3.56	0.886	41.8	4.82	0.413
13.8	3.64	0.851	47.0	4.94	0.385
15.0	3.75	0.804	52.8	5.06	0.358
16.8	3.88	0.745	59.2	5.18	0.335
18.8	4.00	0.690	74.0	5.40	0.294
21.0	4.12	0.641	92.6	5.64	0.259
23.6	4.24	0.593	115.8	5.88	0.228

κ further increases the computational burden and changes L and a by less than 0.1 and 0.5%, respectively.

Our numerical results for L/R are tabulated in Table I and plotted in Figure 2. They are consistent with Helfand's[6] and Shull's[8] results, and with eqs 1 and 31 in the strong and weak segregation limits.

Our numerical results for a/R are tabulated in Table I and plotted in Figure 3. They are consistent with Helfand's[6] and Shull's[8] results, and with eq 2 in the strong segregation limit, and give the expected value $a = 3.23R/\pi$ in the weak segregation limit.

It is comforting that Helfand's results[6] and ours (see Figures 2 and 3) agree, despite our different approaches. Helfand considers ideal Gaussian chains, with $P(\mathbf{r})$

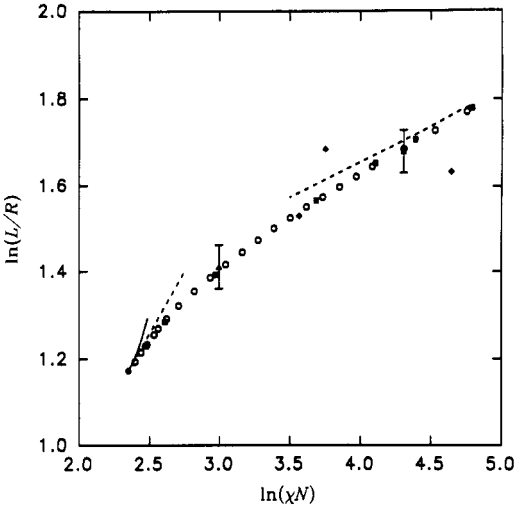

Figure 2. Ratio of lamellar period to radius of gyration versus χN. Our numerical results (Table I) are indicated by open circles, and the filled circle is Leibler's[2] weak segregation limit. The dashed lines are analytic predictions for the weak (eq 31) and strong (eq 1) segregation limits. The calculations of Shull (extracted from Figure 2 of ref 8) are indicated by boxes, those of Helfand[6] by triangles, and the measurements of ref 18 by diamonds. The solid line represents the solution of eq 26.

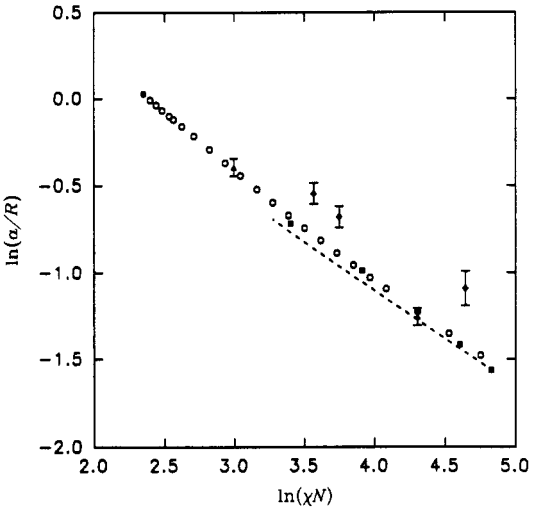

Figure 3. Ratio of interphase width to radius of gyration versus χN. Our numerical results (Table I) are indicated by open circles, and the filled circle is Leibler's[2] weak segregation limit. The dashed line is an analytic prediction for the strong segregation limit (eq 2). The calculations of Shull (extracted from Figure 4 of ref 8) are indicated by boxes, those of Helfand[6] by triangles, and measurements of ref 18 by diamonds.

Gaussian, and approximates the recursion relation (eq 8) by a diffusion differential equation (see eqs II.4 and II.6 of ref 6), while we consider random-walk chains on a lattice, and evaluate the recursion relation directly. We have also investigated the effects of generalizing the random-walk probability distribution of eq B2 to

$$P(z) = \begin{cases} p & \text{if } z = \pm l \\ 1-2p & \text{if } z = 0 \\ 0 & \text{otherwise} \end{cases} \quad (34)$$

where $0 < p \leq 1/2$ and $R^2 = 6pNl^2$ and find that our results are independent of p.

Several measured values[18] of L/R and a/R are also plotted in Figures 2 and 3. The scatter of the L/R values (for which there were no error bars) suggests that theory and experiment agree to within the limit of experimental error. The values of a/R show much less scatter and do not agree with theory. Semenov has recently shown that this

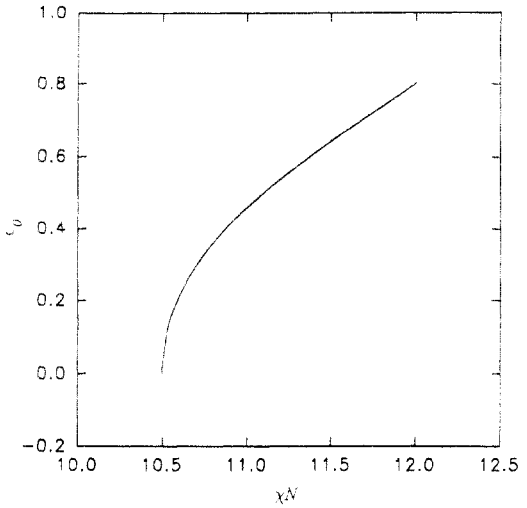

Figure 4. ϵ_0 versus χN from eq 27.

discrepancy can be wholly accounted for by including fluctuation effects, which are neglected in our mean field model.[5]

Analytic predictions for L/R in the weak segregation limit are compared with numerical results in Figure 2. The dashed line representing eq 31 appears to describe the correct limiting behavior as χN approaches the disorder–order transition. However, the solid line representing eq 26 diverges rapidly from our numerical results, which indicates that our free energy expansion (eq 25) is accurate only as $\epsilon \to 0$. Note that the series expansion parameter in eq 25 appears to be $\chi N\epsilon$, not ϵ. Since $\chi N \simeq 10.5$ and ϵ_0 grows very rapidly at the weak segregation limit (see Figure 4), it is understandable that eq 25 converges poorly.

Right at the disorder–order transition our analytic solution gives $\chi N = 10.5$ and $L = 3.23R$, in agreement with Leibler.[2] In his theory of the weak segregation limit, Leibler represents an incompressible melt by imposing the constraint $\phi(\mathbf{r}) = 1$. However, this constraint is not adequate to describe the behavior of L versus χN in the neighborhood of the transition (see eq 19). The $\cos(2qz)$ terms of eqs 17 and 18 contribute to the ϵ^4 terms in the free energy (see terms involving $\tilde{\tau}$ in eq 25) and significantly influence the behavior of L near the weak segregation limit. Excluding the $\cos(2qz)$ terms (set $\tilde{\tau} = a_3 = 0$ in eqs 26–30) gives the limiting behavior $L = 1.442R(\chi N)^{0.343}$, which is quite different than eq 31. As Helfand[6] has emphasized, the ratio $(\phi(\mathbf{r}) - 1)/\kappa$ which appears in eqs 13 and 14 remains finite as $\kappa \to 0$. So the compressibility of the melt must be taken into consideration, even in the limit $\kappa \to 0$, to get the correct dependence of L on χN at the weak segregation limit.

From the order–disorder transition to $\chi N \simeq 13$ the numerical data of Figure 2 appear collinear. Linear regression gives $L \sim R(\chi N)^{0.453}$, consistent with Shull.[8]

In conclusion, we have calculated L and a over the whole range from the weak to the strong segregation limits. Our results are consistent with theoretical formulas in both limits, and agree with those of Shull. Based on the first few terms of a Fourier series expansion of the density profile, we find $L = 0.844R(\chi N)^{0.571}$ at the weak segregation limit; the compressibility of the melt—even in the incompressible limit—must be taken into consideration to get the correct dependence of L on χN, and the Fourier series approximation turns out to be accurate over a very small range of χN.

Acknowledgment. We wish to thank the reviewers for many helpful comments. This work was supported by the NSF materials research group through Grants DMR89-01845 and DMR91-22227.

Appendix A: Evaluation of $\ln(Z_c)$

As in section III.A, consider one-dimensional (lamellar) structure and let $\chi N \simeq 10.5$ as $N \to \infty$ and $\chi \to 0$. We will substitute the approximate expressions for $\mu(A,z)$ and $\mu(B,z)$ from section III.A into the recursion relations for $Z^{\pm}(k,z)$, then calculate approximate expressions for Z_c and $\ln(Z_c)$.

Consider calculating $Z^{\pm}(N/2,z)$ from eq 8. $\mu(B,z)$ is obtained from $\mu(A,z)$ by changing the sign of ϵ, so $Z^+(N/2,z)$ can be obtained from $Z^-(N/2,z)$ in the same way. $\mu(i,z) \sim \chi$ (see eq 20) and $\chi \to 0$, so eq 7 gives

$$Z^0(N/2,z) = Z^-(N/2,z)Z^+(N/2,z) \tag{A1}$$

Then, from eq 6

$$Z_c = \frac{1}{L}\int_0^L Z^-(N/2,z)Z^+(N/2,z)\,dz \tag{A2}$$

Our strategy is to calculate $Z^-(N/2,z)$ from eq 8, change the sign of ϵ to get $Z^+(N/2,z)$, then calculate Z_c from eq A2.

Substituting $\mu(A,z)$ from eq 20 into the exponential in eq 8 and expanding to order ϵ^4 gives

$$e^{-\mu(A,z)} = e^{-\chi/2}\left(1 + \frac{\tilde{\epsilon}^2}{4N^2} + \frac{\tilde{\epsilon}^4}{64N^4} - \frac{\tilde{\tau}\tilde{\epsilon}^4}{8N^3} + \frac{\tilde{\tau}^2\tilde{\epsilon}^4}{4N^2} + \frac{\tilde{\epsilon}}{N}\cos(qz) + \frac{\tilde{\epsilon}^3}{8N^3}\cos(qz) - \frac{\tilde{\tau}\tilde{\epsilon}^3}{2N^2}\cos(qz) + \frac{\tilde{\epsilon}^2}{4N^2}\cos(2qz) - \frac{\tilde{\tau}\tilde{\epsilon}^2}{N}\cos(2qz)\right) \tag{A3}$$

where $\tilde{\epsilon} \equiv \chi N\epsilon/2$, and terms containing $\tilde{\epsilon}^3\cos(3qz)$ and $\tilde{\epsilon}^4\cos(...)$ have been dropped because they contribute terms of higher order than ϵ^4 to the free energy. Motivated by the form of eq A3, write

$$Z^-(k,z) = e^{-\chi(k-1)/2}\left(1 + B_0\frac{\tilde{\epsilon}^2}{4N^2} + B_1\frac{\tilde{\epsilon}^4}{64N^4} - B_2\frac{\tilde{\tau}\tilde{\epsilon}^4}{8N^3} + B_3\frac{\tilde{\tau}^2\tilde{\epsilon}^4}{4N^2} + C_0\frac{\tilde{\epsilon}}{N}\cos(qz) + C_1\frac{\tilde{\epsilon}^3}{8N^3}\cos(qz) - C_2\frac{\tilde{\tau}\tilde{\epsilon}^3}{2N^2}\cos(qz) + D_0\frac{\tilde{\epsilon}^2}{4N^2}\cos(2qz) - D_1\frac{\tilde{\tau}\tilde{\epsilon}^2}{N}\cos(2qz)\right) \tag{A4}$$

where the undetermined coefficients $B_0, B_1, ..., D_1$ are all functions of k, and eq 9 implies that they are all zero for $k = 1$. Substitute from eqs A3 and A4 into both sides of eq 8, perform the summation by using the relation

$$\sum_{z'} P(z' - z)\cos(nqz') = \gamma_n \cos(nqz) \tag{A5}$$

where $P(z)$ is given by eq B2 and $\gamma_n = 1 - n^2\tilde{q}^2/N$, and then equate terms with identical cosine, $\tilde{\tau}$ and $\tilde{\epsilon}$ factors to get recursion relations for the coefficients:

$$B_0(k+1) = 1 + B_0(k) + 2C_0(k) \tag{A6}$$

$$B_1(k+1) = 1 + 4B_0(k) + B_1(k) + 4C_0(k) + 4C_1(k) + 2D_0(k)$$

$$B_2(k+1) = 1 + B_2(k) + 2C_0(k) + 2C_2(k) + D_0(k) + D_1(k)$$

$$B_3(k+1) = 1 + B_3(k) + 2D_1(k)$$

$$C_0(k+1) = \gamma_1(1 + C_0(k))$$

$$C_1(k+1) = \gamma_1(1 + 2B_0(k) + 3C_0(k) + C_1(k) + D_0(k))$$

$$C_2(k+1) = \gamma_1(1 + C_0(k) + C_2(k) + D_1(k))$$

$$D_0(k+1) = \gamma_2(1 + 2C_0(k) + D_0(k))$$

$$D_1(k+1) = \gamma_2(1 + D_1(k))$$

These recursion relations have the general form $X(k+1) = \gamma(X(k) + Y(k))$ with the solution

$$X(k) = -Y(k) + \gamma^k \sum_{n=1}^{k} \gamma^{-n} Y(n) \tag{A7}$$

from which the coefficients can be determined as functions of k. For example, to evaluate $C_0(k)$ take $\gamma = \gamma_1$ and $Y(k) = 1$, then eq A7 gives

$$\begin{aligned} C_0(k) &= -1 + \gamma_1{}^k \sum_{n=1}^{k} \gamma_1{}^{-n} \\ &= -1 + \frac{1 - \gamma_1{}^{-k}}{1 - \gamma_1{}^{-1}} \\ &= -1 + \frac{N}{\tilde{q}^2} - \frac{\gamma_1^k N}{\tilde{q}^2} \end{aligned} \tag{A8}$$

The other coefficients are computed in a similar fahsion, but the results are lengthy and are omitted here. Equation A4 gives

$$\begin{aligned} Z^-(N/2,z) = e^{-\chi N/4}\Bigg(1 + \tilde{B}_0\frac{\tilde{\epsilon}^2}{4} + \tilde{B}_1\frac{\tilde{\epsilon}^4}{64} - \tilde{B}_2\frac{\tilde{\tau}\tilde{\epsilon}^4}{8} + \tilde{B}_3\frac{\tilde{\tau}^2\tilde{\epsilon}^4}{4} + \\ \tilde{C}_0\tilde{\epsilon}\cos(qz) + \tilde{C}_1\frac{\tilde{\epsilon}^3}{8}\cos(qz) - \tilde{C}_2\frac{\tilde{\tau}\tilde{\epsilon}^3}{2}\cos(qz) + \\ \tilde{D}_0\frac{\tilde{\epsilon}^2}{4}\cos(2qz) - \tilde{D}_1\tilde{\tau}\tilde{\epsilon}^2\cos(2qz)\Bigg) \end{aligned} \tag{A9}$$

where $\tilde{B}_0 \equiv B_0(N/2)/N^2$, $\tilde{B}_1 \equiv B_1(N/2)/N^4$, and so forth, and we evaluate everything in the limit $N \to \infty$. Continuing the previous example (see eq A8)

$$\begin{aligned} \tilde{C}_0 &\equiv C_0(N/2)/N \\ &= -\frac{1}{N} + \frac{1}{\tilde{q}^2} - \frac{\gamma_1^{N/2}}{\tilde{q}^2} \\ &\to \frac{1}{\tilde{q}^2} - \frac{y}{\tilde{q}^2} \end{aligned} \tag{A10}$$

where $y \equiv e^{-\tilde{q}^2/2}$. The other coefficients are computed in a similar fashion, giving

$$\tilde{B}_0 = \frac{1}{\tilde{q}^2} - \frac{2}{\tilde{q}^4} + \frac{2y}{\tilde{q}^4} \tag{A11}$$

$$\tilde{B}_1 = \frac{2}{\tilde{q}^4} - \frac{15}{\tilde{q}^6} - \frac{20y}{3\tilde{q}^6} + \frac{87}{2\tilde{q}^8} - \frac{392y}{9\tilde{q}^8} + \frac{y^4}{18\tilde{q}^8}$$

$$\tilde{B}_2 = \frac{3}{2\tilde{q}^4} + \frac{y}{\tilde{q}^4} - \frac{21}{4\tilde{q}^6} + \frac{16y}{3\tilde{q}^6} - \frac{y^4}{12\tilde{q}^6}$$

$$\tilde{B}_3 = \frac{1}{4\tilde{q}^2} - \frac{1}{8\tilde{q}^4} + \frac{y^4}{8\tilde{q}^4}$$

$$\tilde{C}_0 = \frac{1}{\tilde{q}^2} - \frac{y}{\tilde{q}^2}$$

$$\tilde{C}_1 = \frac{2}{\tilde{q}^4} + \frac{5y}{3\tilde{q}^4} - \frac{15}{2\tilde{q}^6} + \frac{68y}{9\tilde{q}^6} - \frac{y^4}{18\tilde{q}^6}$$

$$\tilde{C}_2 = -\frac{y}{2\tilde{q}^2} + \frac{5}{4\tilde{q}^4} - \frac{4y}{3\tilde{q}^4} + \frac{y^4}{12\tilde{q}^4}$$

$$\tilde{D}_0 = \frac{1}{2\tilde{q}^4} - \frac{2y}{3\tilde{q}^4} + \frac{y^4}{6\tilde{q}^4}$$

$$\tilde{D}_1 = \frac{1}{4\tilde{q}^2} - \frac{y^4}{4\tilde{q}^2}$$

Equation A9 is an approximation for $Z^-(N/2,z)$, and $Z^+(N/2,z)$ is obtained by chaning the sign of ϵ. Substituting these expressions into eq A2, integrating, and keeping terms up to ϵ^4, gives

$$\begin{aligned} Z_c = e^{-\chi N/2}(1 + a_1(\chi N)^2\epsilon^2 + \\ (a_2 + a_3\tilde{\tau} + a_4\tilde{\tau}^2)(\chi N)^4\epsilon^4) \end{aligned} \tag{A12}$$

where

$$a_1 \equiv (\tilde{B}_0 - \tilde{C}_0{}^2)/8 \tag{A13}$$

$$a_2 \equiv (2\tilde{B}_0{}^2 + \tilde{B}_1 - 4\tilde{C}_0\tilde{C}_1 + \tilde{D}_0{}^2)/512$$

$$a_3 \equiv (-\tilde{B}_2 + 2\tilde{C}_0\tilde{C}_2)/64$$

$$a_4 \equiv (\tilde{B}_3 + \tilde{D}_1{}^2)/32$$

Equation A12 is an approximation for Z_c in the weak segregation limit ($\epsilon \to 0$), from which $\ln(Z_c)$ is readily calculated.

Appendix B: Numerical Solution in One Dimension

To specialize to the case of one-dimensional (lamellar) structure and symmetric blocks, replace the lattice vector $\mathbf{r}$ by one component, let

$$i_k = \begin{cases} A \text{ if } k \le N/2 \\ B \text{ if } k > N/2 \end{cases} \tag{B1}$$

$$P(z) = \begin{cases} 1/6 & \text{if } z = \pm l \\ 4/6 & \text{if } z = 0 \\ 0 & \text{otherwise} \end{cases} \tag{B2}$$

and seek solutions $\phi(i,z)$ and $\mu(i,z)$ periodic in z with period L. (Keep in mind that z is a discrete variable, and ϕ and μ are discrete distributions.) Because the blocks are symmetric, $\phi(A,z) = \phi(B,z+L/2)$ and $\mu(A,z) = \mu(B,z+L/2)$, and knowledge of the solution over any half-period determines the entire solution. Specifically, let $z = jl$, where $j = 1, 2, \ldots, \mathcal{N}$ and $\mathcal{N} = L/(2l)$, and impose the "reflecting wall" boundary conditions (required to evaluate the convolutions in eq 8)

$$\mu(i,0) = \mu(i,l) \tag{B3}$$

$$\mu(i,L/2+l) = \mu(i,L/2) \tag{B4}$$

$L/(2l)$ must be an integer, and the center of the interphase region is at $L/4$.

The solution proceeds as follows: Given χ, N, κ, and $\mathcal{N}$, and given an initial guess for $\phi(i,z)$, iterate until Δ is within a specified tolerance (typically 0.001) of zero, and calculate the free energy from eq 12. Then select a new value of $\mathcal{N}$, reinitialize $\phi(i,z)$, and repeat the procedure. Keep this up until the value of $\mathcal{N}$ which minimizes the free energy is determined. The corresponding $\phi(i,z)$ is the equilibrium density distribution, with period $L = 2\mathcal{N}l$ and interphase

width

$$a = \frac{\phi(A,L/2) - \phi(A,l)}{\phi'(A,L/4)} \tag{B5}$$

where ϕ' represents the derivative with respect to z and is evaluated by fitting a natural cubic spline to $\phi(A,z)$. In practice, we find the three even and three odd values of $\mathcal{N}$ which bracket the minimum free energy, calculate the corresponding values of L and a, then use parabolic interpolation to estimate their values at the minimum free energy. The even and odd data sets are treated separately, and their results compared. If they disagree, then this means the lattice is too coarse to accurately describe the narrow interphase region. The solution is to increase the number of molecular segments N, which effectively decreases the segment length (and lattice constant) l. But increasing N increases the computational burden. For each data point in Table I, N was made large enough so that the even and odd results agreed to within 0.7% for L and 3.3% for a.

The initial density distribution we use is

$$\phi(A,z) = 1 - \phi(B,z) = \Theta(L/4-z) \tag{B6}$$

where $\Theta(z)$ is the unit step function. However, for small κ the iterative procedure fails (Δ does not go to zero). The solution is to start with a relatively large value of κ (typically 10), solve for $\phi(i,z)$, then use this as a new initial distribution with a (typically 5%) smaller value of κ. We proceed in this way until we reach the desired value κ = 0.1.

References and Notes

(1) Bates, F. S. *Science* **1991**, *251*, 898.
(2) Leibler, L. *Macromolecules* **1980**, *13*, 1602.
(3) Semenov, A. N. *Sov. Phys. JETP* **1985**, *61*, 733.
(4) Helfand, E.; Tagami, Y. *J. Chem. Phys.* **1972**, *56*, 3592.
(5) Semenov, A. N. Theory of Block-Copolymer Interfaces in Strong Segregation Limit. Submitted to *Macromolecules*.
(6) Helfand, E. *Macromolecules* **1975**, *8*, 552. Results for L and a were extracted from Figures 2 and 3, with an estimated uncertainty of ±5%.
(7) Melenkevitz, J.; Muthukumar, M. *Macromolecules* **1991**, *24*, 4199.
(8) Shull, K. R. *Macromolecules* **1992**, *25*, 2122.
(9) Ohta, T.; Kawasaki, K. *Macromolecules* **1986**, *19*, 2621.
(10) Almdal, K.; Rosedale, J. H.; Bates, F. S.; Wignall, G. D.; Fredrickson, G. H. *Phys. Rev. Lett.* **1990**, *65*, 1112.
(11) Olvera de la Cruz, M. *Phys. Rev. Lett.* **1991**, *67*, 85.
(12) Helfand, E. *J. Chem. Phys.* **1975**, *62*, 999.
(13) de Gennes, P. G. *Scaling Concepts in Polymer Physics*; Cornell University Press: Ithaca, NY, 1979; pp 29–31.
(14) Helfand, E.; Wasserman, Z. R. *Macromolecules* **1976**, *9*, 879.
(15) Feynman, R. P. *Statistical Mechanics*; W. A. Benjamin, Inc.: Reading, MA, 1972; pp 67–70.
(16) Press, W. H.; Flannery, B. P.; Teukolsky, S. A.; Vetterling, W. T. *Numerical Recipes in C*; Cambridge University Press: Cambridge, 1990; p 317.
(17) Press, W. H.; Flannery, B. P.; Teukolsky, S. A.; Vetterling, W. T. *Numerical Recipes in C*; Cambridge University Press: Cambridge, 1990; p 299.
(18) Anastasiadis, S. H.; Russell, T. P.; Satija, S. K.; Majkrzak, C. F. *J. Chem. Phys.* **1990**, *92*, 5677.